

ADA 080 918

TECHNICAL
LIBRARY



TECHNICAL REPORT RL-80-3

**IMPROVING A REAL TIME ACOUSTICAL
HOLOGRAPHIC SYSTEM FOR FLAW DETECTION**

W. F. Swinson
Auburn University
Auburn, Alabama
for
Ground Equipment and Missile Structures Directorate
US Army Missile Laboratory

1 October 1979



U.S. ARMY MISSILE COMMAND

Redstone Arsenal, Alabama 35809

Approved for public release; distribution unlimited.

DISPOSITION INSTRUCTIONS

DESTROY THIS REPORT WHEN IT IS NO LONGER NEEDED. DO NOT RETURN IT TO THE ORIGINATOR.

DISCLAIMER

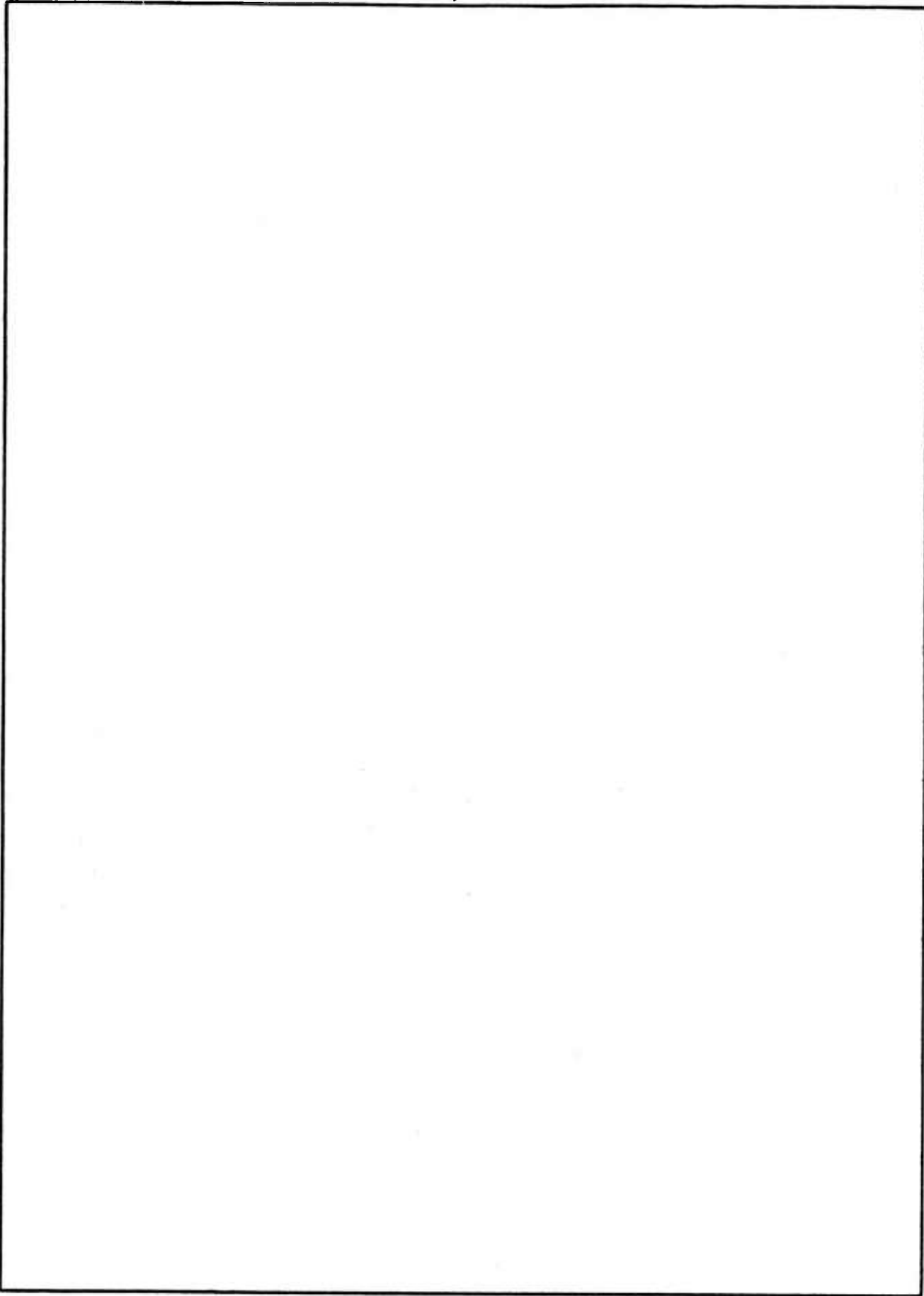
THE FINDINGS IN THIS REPORT ARE NOT TO BE CONSTRUED AS AN OFFICIAL DEPARTMENT OF THE ARMY POSITION UNLESS SO DESIGNATED BY OTHER AUTHORIZED DOCUMENTS.

TRADE NAMES

USE OF TRADE NAMES OR MANUFACTURERS IN THIS REPORT DOES NOT CONSTITUTE AN OFFICIAL ENDORSEMENT OR APPROVAL OF THE USE OF SUCH COMMERCIAL HARDWARE OR SOFTWARE.

REPORT DOCUMENTATION PAGE		READ INSTRUCTIONS BEFORE COMPLETING FORM
1. REPORT NUMBER RL -80-3	2. GOVT ACCESSION NO.	3. RECIPIENT'S CATALOG NUMBER
4. TITLE (and Subtitle) IMPROVING A REAL TIME ACOUSTICAL HOLOGRAPHIC SYSTEM FOR FLAW DETECTION	5. TYPE OF REPORT & PERIOD COVERED Technical Report	6. PERFORMING ORG. REPORT NUMBER
		7. AUTHOR(s) W. F. Swinson (Auburn University)
9. PERFORMING ORGANIZATION NAME AND ADDRESS Commander US Army Missile Command ATTN: DRSMI-RL Redstone Arsenal, Alabama 35809	10. PROGRAM ELEMENT, PROJECT, TASK AREA & WORK UNIT NUMBERS	8. CONTRACT OR GRANT NUMBER(s)
11. CONTROLLING OFFICE NAME AND ADDRESS Commander US Army Missile Command ATTN: DRSMI-RPT Redstone Arsenal, Alabama 35809	12. REPORT DATE 1 October 1979	15. SECURITY CLASS. (of this report) Unclassified
	13. NUMBER OF PAGES 34	15a. DECLASSIFICATION/DOWNGRADING SCHEDULE
14. MONITORING AGENCY NAME & ADDRESS (if different from Controlling Office)	16. DISTRIBUTION STATEMENT (of this Report) Approved for public release; distribution unlimited.	
17. DISTRIBUTION STATEMENT (of the abstract entered in Block 20, if different from Report)		
18. SUPPLEMENTARY NOTES This work was accomplished through the Laboratory Research Cooperative Program (LRCP) between Dr. W. F. Swinson of the Department of Mechanical Engineering, Auburn University, and the US Army Missile Command.		
19. KEY WORDS (Continue on reverse side if necessary and identify by block number) Real Time Optical Reconstruction Acoustical Holography Flaw Detection Thermoplastic Spatial Filter		
20. ABSTRACT (Continue on reverse side if necessary and identify by block number) This report documents work performed to improve the acoustical imaging capability of an acoustical holographic system for flaw detection. Included in the report is a mathematical model of the acoustical system and the results of the experimental effort to improve it. Added improvements include new plexiglas acoustical lenses, a lens gymbal mount, object gymbal mount, and acoustical thermoplastic memory. An attempt to use glycerine as a new acoustical couplant media is also reported. Work is also reported about the generation of acoustical real time speckle interferograms using the system.		

SECURITY CLASSIFICATION OF THIS PAGE(When Data Entered)



SECURITY CLASSIFICATION OF THIS PAGE(When Data Entered)

CONTENTS

Section	Page
I. Introduction	5
II. Theory	5
III. Experimentation	13
IV. Conclusions and Recommendations	26

ILLUSTRATIONS

Figure	Page
1. Acoustical Holography Layout	6
2. Acoustical Surface	7
3. Diffraction Orders	11
4. Object Beam Only	12
5. Hologram from Higher Order Diffraction Patterns	12
6. Plexiglas Lens and Holder	14
7. Test Target	14
8. Flaw Model	15
9. Test Target Acoustical Hologram	17
10. Magnified Test Target Hologram	17
11. Flaw Model Hologram	18
12. Magnified Flaw Hologram	18
13. Acoustical Reflector	19
14. Model Traverse	19
15. Sealed Transducer	21

ILLUSTRATIONS (Concluded)

Figure	Page
16. Resistance Heated Thermoplastic Device	21
17. Resistance Heating Circuit	23
18. Filtered Observation	24
19. Floating Thermoplastic Device	24
20. Film Filter System	25
21. Film Record	25
22. Acoustical Young's Fringes	26

I. INTRODUCTION

The objective of the effort reported in this report was to improve the capability of the real time acoustical holographic system to detect, locate, and size subsurface flaws in missile components.

The basic system is shown in *Figure 1*. A discussion of this system is included in a report from Irelan, et al. [1]

II. THEORY

A mathematical model is included in this report to assist in understanding the acoustical system. Consider the surface of the water shown in *Figure 2*; the surface disturbance, \bar{P}_{AO} , due to the object wave is (note: only the real part of the complex quantities represent the disturbances)

$$\bar{P}_{AO} = \bar{P}_O e^{i(w_A t + \phi_{AO})} \quad (1)$$

where

\bar{P}_O = the maximum amplitude of the object wave at the fluid surface (related to pressure induced into the model and model characteristics)

w_A = acoustic frequency, and

ϕ_{OA} = acoustic phase of object wave arriving at surface and is a function of x, y.

The disturbance of the surface due to the reference wave is

$$\bar{P}_{AR} = \bar{P}_R e^{i(w_A t + \phi_{AR})} \quad (2)$$

where

\bar{P}_R = maximum amplitude of the reference wave.

ϕ_{AR} = acoustic phase of the reference wave at the water surface and is a function of x, y.

1. Irelan, V.G., Mullinix, B. R., Castle, J. G., "Real Time Acoustical Holography Systems," US Army Missile Research and Development Command, Technical Report T-78-10, Redstone Arsenal, Alabama 35809, October 1977.

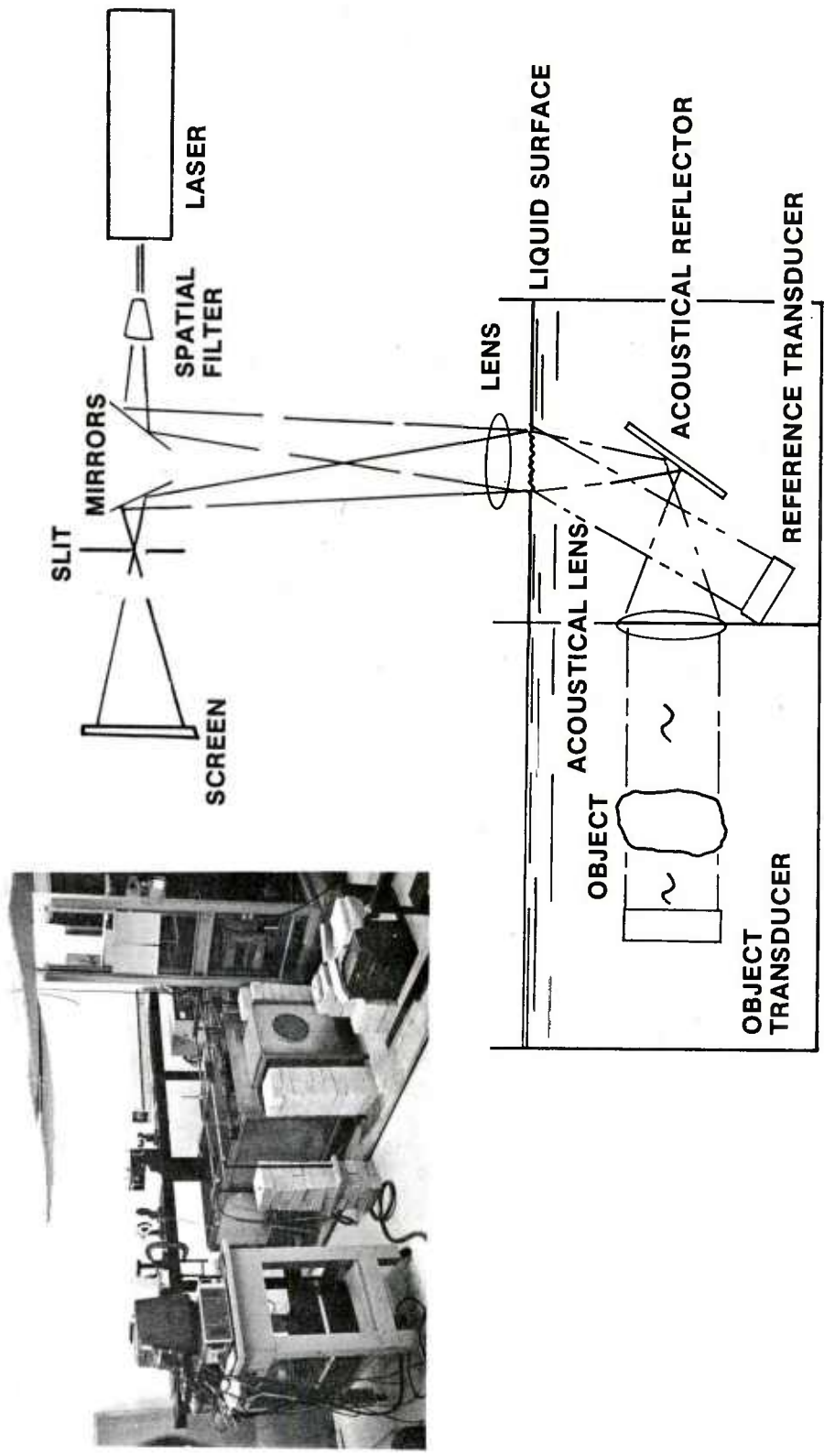
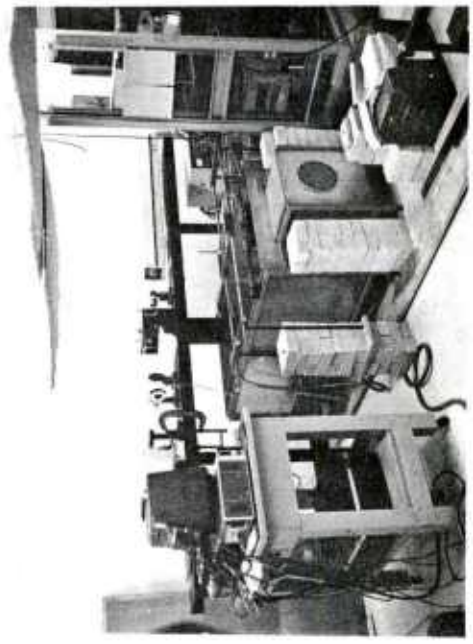


Figure 1. Acoustical holography layout.



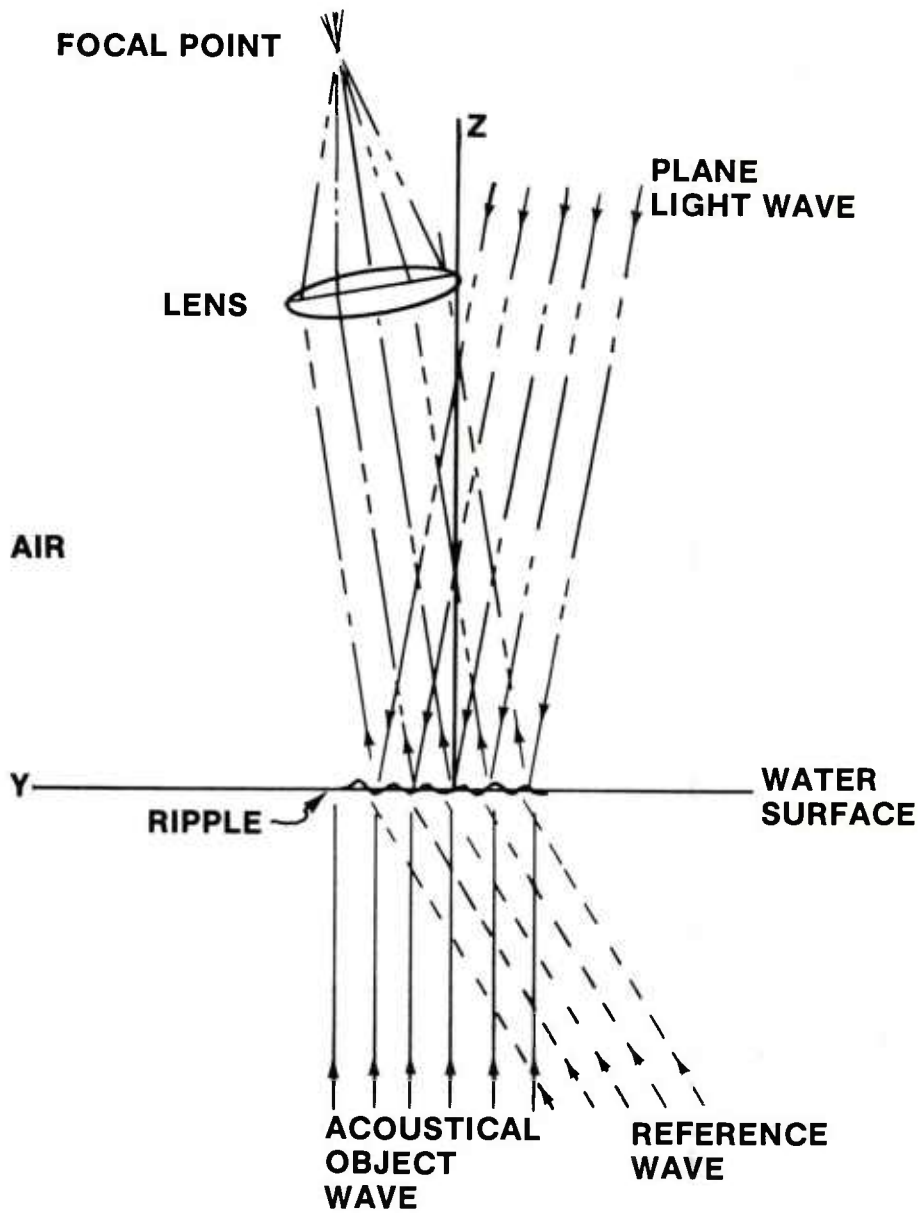


Figure 2. Acoustical surface.

The resulting surface disturbance due to the two disturbances interfering is

$$\bar{P} = \bar{P}_{AO} + \bar{P}_{AR} \quad (3)$$

The total disturbance intensity (which is proportional to the ripple height on the surface) is

$$I = \bar{P} \cdot \bar{P}^* \quad (4)$$

where (*) denotes the complex conjugate. Equation (4) in expanded form is

$$I = \left[\bar{P}_O e^{i(w_A t + \phi_{AO})} + \bar{P}_R e^{i(w_A t + \phi_{AR})} \right] \cdot \left[\bar{P}_O e^{-i(w_A t + \phi_{AO})} + \bar{P}_R e^{-i(w_A t + \phi_{AR})} \right]$$

or

$$I = P_O^2 + P_R^2 + P_O P_R e^{i(\phi_{AO} - \phi_{AR})} + P_O P_R e^{-i(\phi_{AO} - \phi_{AR})} \quad (5)$$

With the assumption that the surface displacement is proportional to the disturbance intensity, then

$$Z = C_1 \left[P_O^2 + P_R^2 + 2 P_O P_R \cos (\phi_{AO} - \phi_{AR}) \right] \quad (6)$$

One "ray" of light at the lens focal point changes its path length by 2Z (assuming small incident and reflecting angles); thus the optical disturbance at the focal point is

$$\bar{E} = \bar{A} e^{i(w_L t + \phi_L)} e^{i4\pi Z/\lambda_L} \quad (7)$$

where

\bar{A} = maximum amplitude of the optical disturbance,

w_L = light wave frequency,

ϕ_L = light wave phase, and

λ_L = light wave length.

Equation (7) in expanded form is

$$\begin{aligned} \bar{E} = \bar{A} e^{i(w_L t + \phi_L)} e^{i(4\pi/\lambda_L)} P_O^2 + \\ P_R^2 + 2P_O P_R \cos(\phi_{AO} + \phi_{AR}) C_1 \end{aligned} \quad (8)$$

To assist in interpreting this result the Bessel identity

$$e^{i x \cos \theta} = \sum_{n=-\infty}^{\infty} i^n j_n(x) e^{-i n \theta} \quad (9)$$

is helpful. Thus Equation (8) becomes

$$\begin{aligned} \bar{E} = \bar{A} e^{i(w_L t + \phi_L)} e^{i(4\pi/\lambda_L)} (P_O^2 + P_R^2) C_1 \sum_{n=-\infty}^{\infty} i^n j_n \\ \cdot \left[C_1 (8\pi/\lambda_L) P_O P_R \right] e^{-i n (\phi_{AO} - \phi_{AR})} \end{aligned} \quad (10)$$

with "n" denoting diffraction orders 0, ± 1, ± 2, -----.

The diffraction orders are

$$\begin{aligned} \bar{E}_0 = \bar{A} e^{i(w_L t + \phi_L)} e^{i(4\pi/\lambda_L)} (P_O^2 + P_R^2) C_1 j_0 \\ \cdot \left[C_1 (8\pi/\lambda_L) P_O P_R \right] \\ \bar{E}_1 = \bar{A} e^{i(w_L t + \phi_L)} e^{i C_1 (4\pi/\lambda_L)} (P_O^2 + P_R^2) i j_1 \\ \cdot \left[C_1 (8\pi/\lambda_L) P_O P_R \right] e^{-i(\phi_{AO} - \phi_{AR})} \end{aligned} \quad (11)$$

•
•
•

Hildebrand and Brenden "Introduction to Acoustical Holography," New York: Plenum Press, 1972 suggest that the argument of the Bessel function, $C_1(8\pi/\lambda_L) P_O P_R$, is very small in which case j_0 approaches "1" and j_1 approaches the argument value of $C_1(8\pi/\lambda_L) P_O P_R$. This result seems plausible as diffraction orders can be seen at the focal plane and are illustrated in *Figure 3*. With the above assumption

$$\begin{aligned} \bar{E}_O &= \bar{A} e^{i(w_L t + \phi_L)} e^{i(4\pi/\lambda_L) C_1(P_O^2 + P_R^2)} \\ \bar{E}_1 &= i \bar{A} e^{i(w_L t + \phi_L)} e^{i(4\pi/\lambda_L) C_1(P_O^2 + P_R^2)} \\ &\quad \cdot [C_1(\pi 8/\lambda_L) P_O P_R] e^{-i(\phi_{AO} - \phi_{AR})} \end{aligned} \quad (12)$$

•
•
•

the intensities are

$$\begin{aligned} I_O &= A^2 \\ I_1 &= A^2 C_1(\pi 8/\lambda_L) P_R^2 + P_O^2 \end{aligned} \quad (13)$$

•
•
•

The predictions from Equation (13) suggest that the zero order does not contain information directly proportional to the acoustic object beam. However, recall that the mathematical description is for one "ray" and, since the surface ripple modulates the light beam, then some information relative to the object would be expected in the zero order beam. In blocking the zero order, the other diffraction orders are directly proportional to the acoustic object beam intensity as seen from Equation (13). Note that without an acoustic reference no diffractions orders are predicted, which is observed experimentally. *Figure 4* is the result of the zero order beam with no reference of two bars. For this result the object power was fully on. *Figure 5* is the result of blocking the zero order beam and including a reference beam. The object power for this was about one half maximum. There is some argument that *Figure 4* is a Gabor hologram, but the size is distorted and may only be an obstruction to the object transducer.

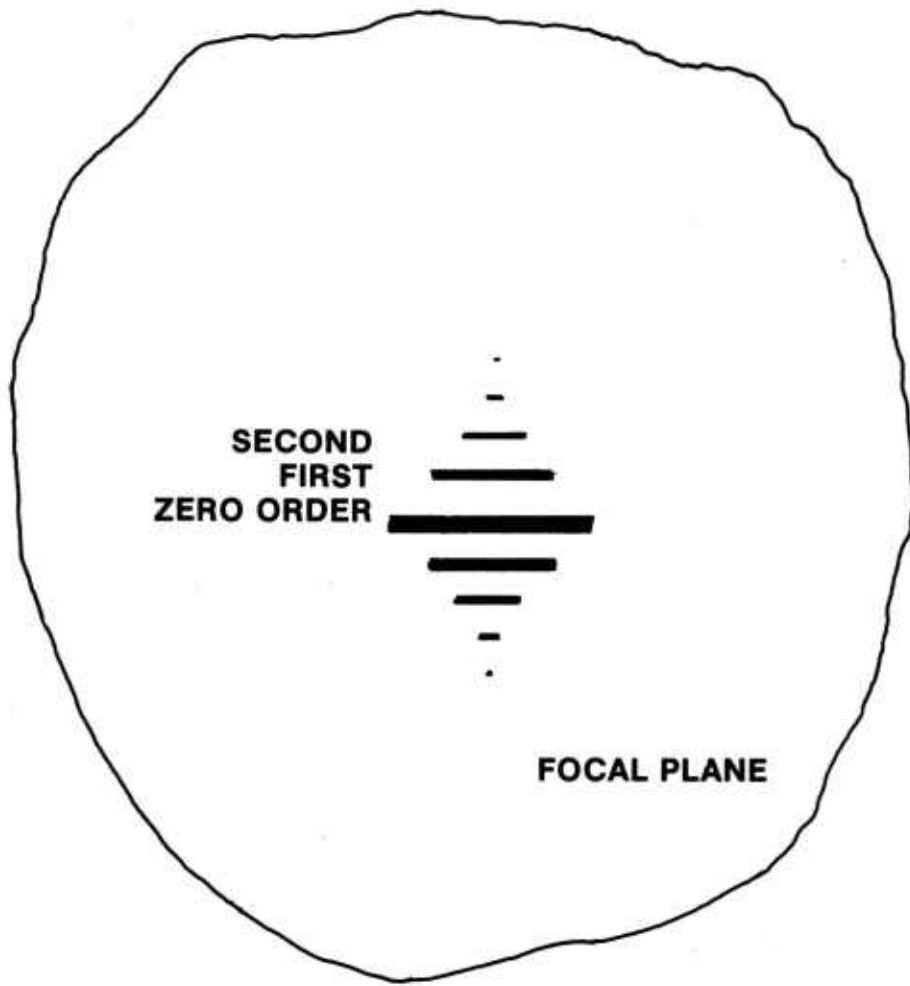


Figure 3. Diffraction orders.

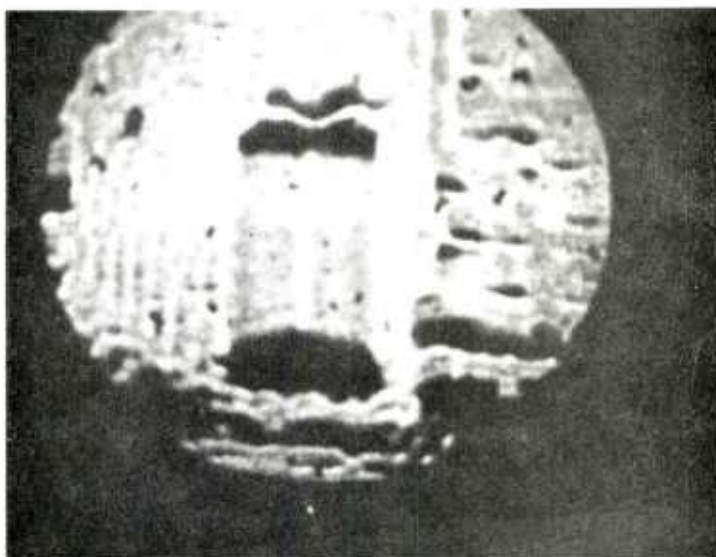


Figure 4. Object beam only.

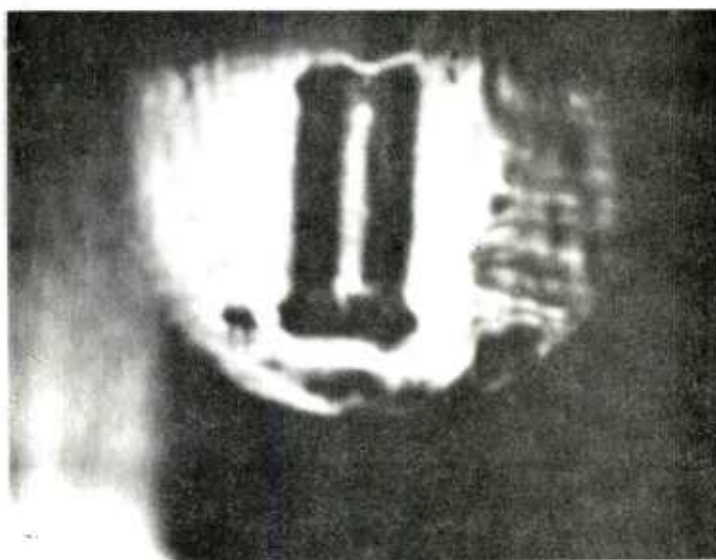


Figure 5. Hologram from higher order diffraction patterns.

III. EXPERIMENTATION

A couplant other than water was investigated. Glycerine was the material investigated. In going from water to steel 86 percent of the energy is reflected and 14 percent transmitted. In going from glycerine to steel 78 percent is reflected and 22 percent is transmitted. These numbers are for normal incidence. This suggests that 50 percent more transmitted energy is present in a model when using glycerine rather than water as an immersion fluid. This was experienced in trying the glycerine as an immersion fluid; however, the surface tension was so much greater than water that a ripple pattern on the surface could not be imaged. The glycerine was mixed with water and at 30 percent glycerine, ripple patterns were evident on the surface; however another problem came up. Even though the mixture looked uniform, when imaging the object dark and bright lines there was considerable scatter of the acoustical beam since the water and glycerine did not form a homogeneous mixture. There is still the possibility of adding detergent to reduce surface tension and promote a homogeneous mixture. This was not tried due to the lack of time. The glycerine had some beneficial effects in that it prevented rust and also damped out fluid motion. Another suggestion would be to try ethylene glycol; while it does not significantly increase the transmitted energy, it does retard rust.

A different lens was tried. Two lenses were made from plexiglas. The lenses were flat on one side and spherically concave on the other side. The concept for this design was to increase the energy input through the lens by having one surface the flat surface, and the first surface essentially perpendicular to the acoustical beam propagation path. Also lens distortion would be less because of the rigidity of the lens compared to a liquid lens. One lens had a radius of curvature of 2.250 inches and the other 4.50 inches. One of the lens and its holder is shown in *Figure 6*. To illustrate the use of the lens and other concepts in this report a target shown in *Figure 7* was used. The bars are approximately 1.5 inches long and the wider bars are about 0.35 inch wide. The target consists of black paper tape like material for the bars glued on a 0.25 inch thick piece of plexiglas. Also a flaw type model is used in some later examples. The flaw model is shown in *Figure 8* and consists of a "teflon flaw" about .5 inch by one inch sandwiched between steel and a slip silica material. The steel is five inches by five inches by 0.1 inch and is bonded to a five inch by five inch by 0.4 inch silica material.

Note that the lens holder has the capability of motion or adjustment in three directions and also rotation about the vertical axis. This holder allows the lens to be adjusted to its aligned position. Further, some control is possible on the object distance and image distance from the lens. The focal point for the acoustical lens can be calculated from thin lens equation

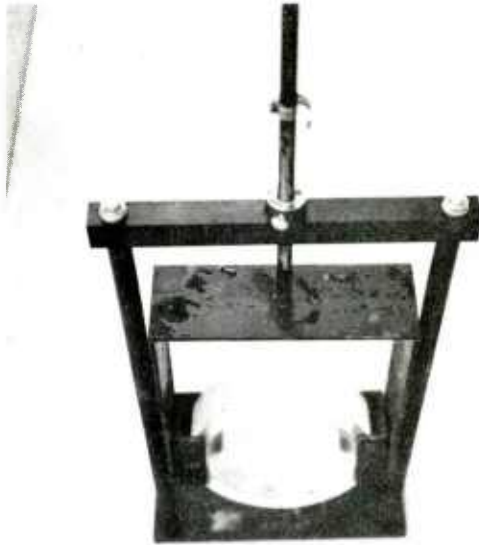


Figure 6. Plexiglas lens and holder.

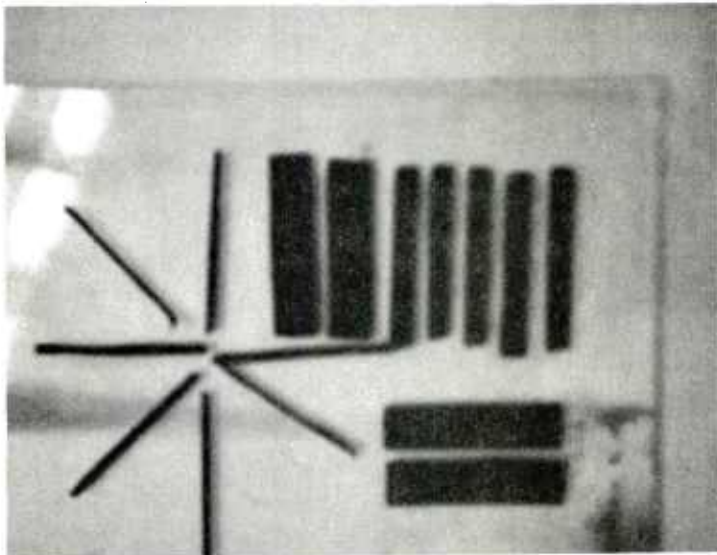


Figure 7. Test target.

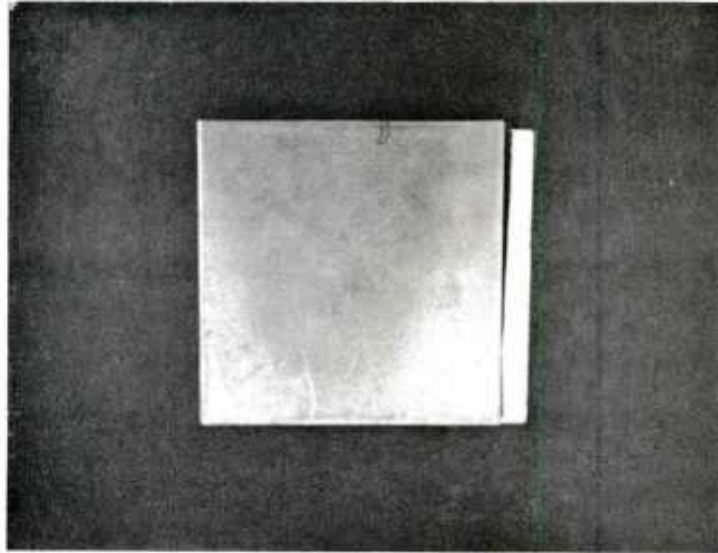


Figure 8. Flaw model.

$$1/f = (n - 1) (1/R_1 - 1/R_2) \quad (14)$$

where

f = lens focal length

R_1 = radius of curvature of first surface (which is infinite for the plexiglas lens)

R_2 = radius of curvature for second surface (which is -2.250 inches and -4.5 inches for the two plexiglas lenses)

n = index of refraction which is $(v_{\text{water}}/v_{\text{plexiglas}})$

v_{water} = longitudinal velocity of sound of immersion fluid (4,863 ft/sec for water)

$v_{\text{plexiglas}}$ = longitudinal velocity of sound in lens material (8,760 ft/sec for plexiglas)

For the 2,250 inches radius lens, the focal length, f , is 5.1 inches. For the 4.50 inches radius lens the focal length, f , is 10.2 inches. The approximate distance of the object and image distance from the lens is calculated from the very familiar thin lens equation

$$1/s + 1/s' = 1/f \quad (15)$$

where

s = the distance of object from lens and

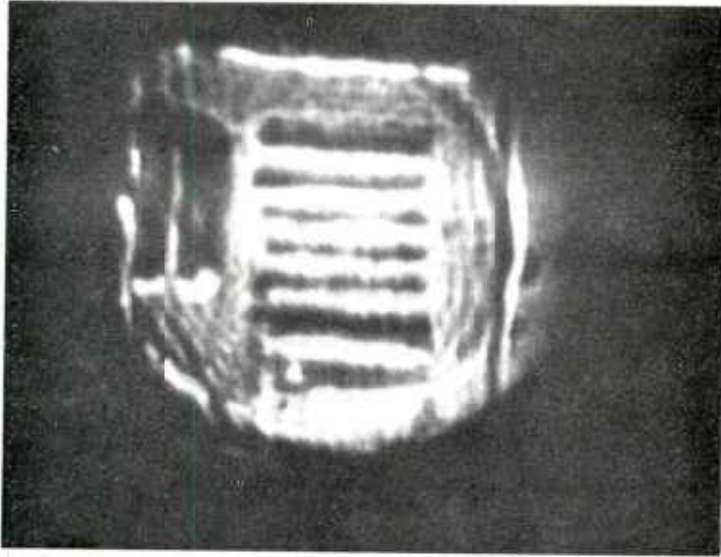
s' = the distance of image from lens.

The performance of the lenses was judged to be an improvement over other lenses. First the field of interference was reasonably uniform, which was not achieved with the other lenses. There appeared to be less distortion of the image with the more rigid plexiglas lens. Of significant note was the increase in resolution when the 5.1 inches focal length lens was used with magnification. The test target hologram is shown in *Figure 9* using the 10.2 inches focal length lens. *Figure 10* using the shorter focal length lens and magnification indicates the increased resolution. *Figures 11* and *12* show the flawed model. The surface tilt as noted in previous reports is very important in being able to "see" the flaw.

It is recommended that improvement in the imaging of flaws can be achieved by image enhancement such as mentioned in imaging some space pictures. This could be incorporated into the system on a real time basis by digitizing the screen image (*Figure 1*), enhancing the image with digital filtering and then playing the information back on a TV screen. The equipment basic to this procedure seems to be available in-house.

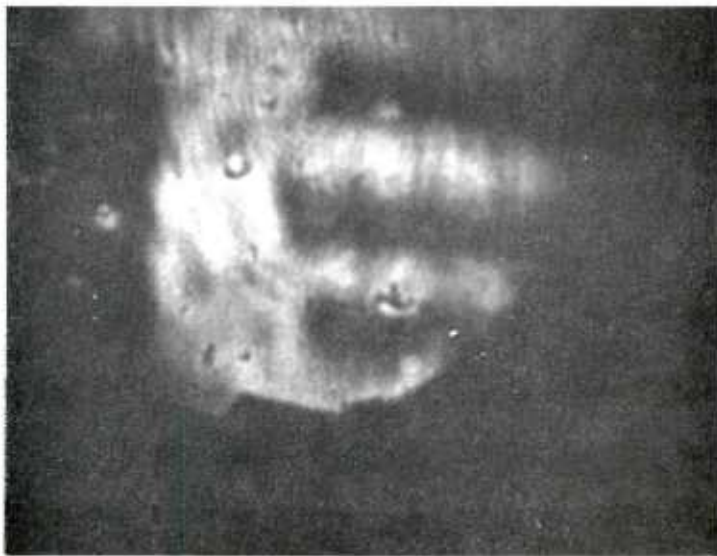
To improve the image an acoustical reflector of stainless polished steel was inserted into the system (*Figure 13*). This did improve the image quality and seemed to reduce stray reflections. Steel has a higher acoustic impedance than most other readily available materials such as aluminum, glass or brass. However, tungsten has an acoustic impedance of twice that of steel which depending on availability and cost would make an excellent reflector.

Another item to improve the acoustical system was the use of a freestanding model holder. With the holder pictured in *Figure 14*, a model can be translated in three orthogonal directions very conveniently. The model can also be rotated about the vertical axis to assist in "seeing through" models at critical angles. The frame needs to be a little more rigid. Also a thin



LENS: $f = 10.2''$ $S = 24$
LASER: 150 MW
OBJ. POWER 3/4
REF. POWER 1/4

Figure 9. Test target acoustical hologram.



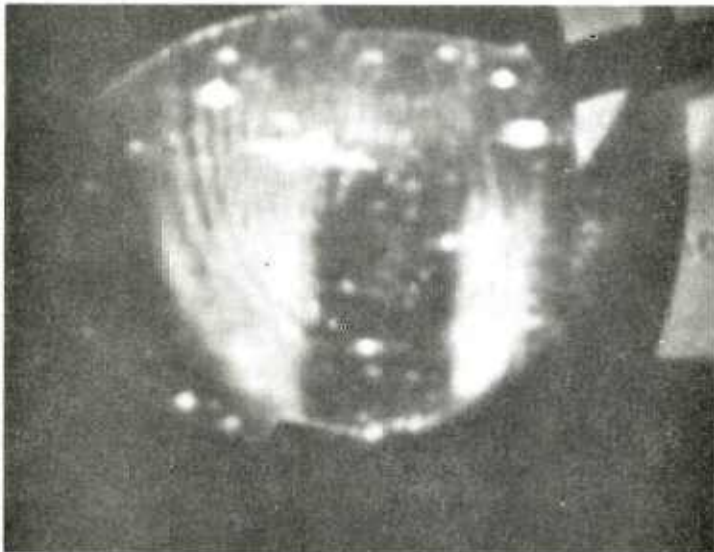
LENS: $f = 5.1$ $S = 7''$
LASER: 150 MW
OBJ. POWER 3/4
REF. POWER 3/8

Figure 10. Magnified test target hologram.



LENS: $f = 10.2''$ $S = 24''$
LASER: 150 MW
OBJ. POWER 4/4
REF. POWER 3/8

Figure 11. Flaw model hologram.



LENS: $f = 5.1''$ $S = 7''$
LASER: 150 MW
OBJ. POWER 4/4
REF. POWER 3/8

Figure 12. Magnified flaw hologram.

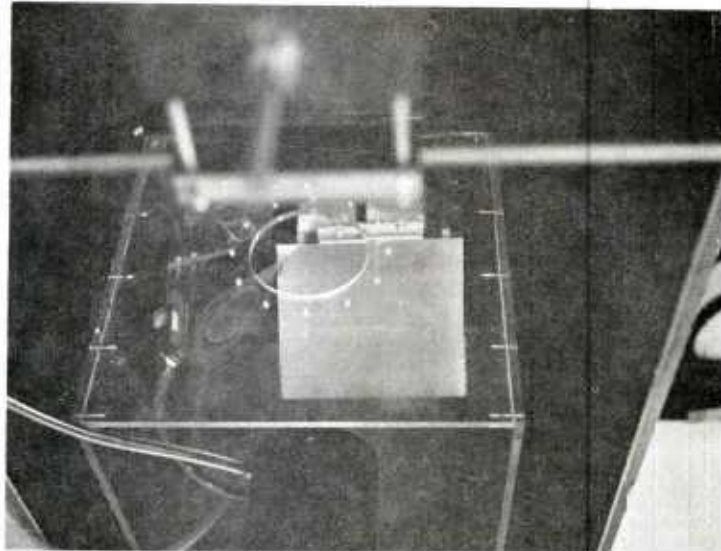


Figure 13. Acoustical reflector.

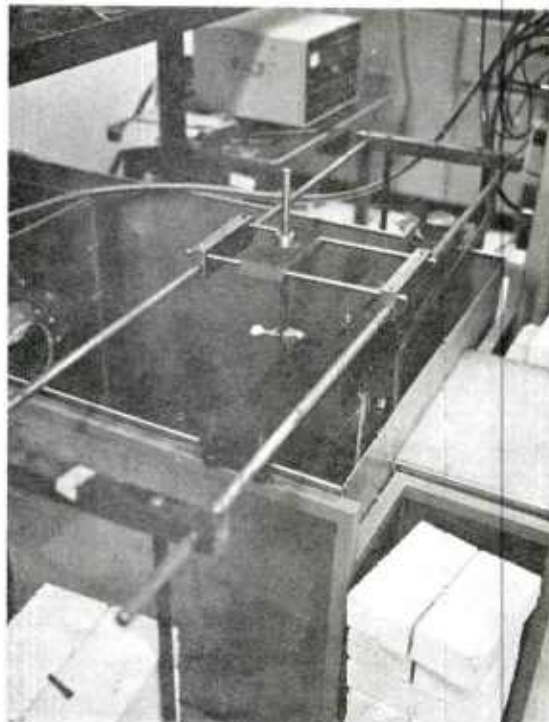


Figure 14. Model traverse.

membrane over the opening in the isolation tank (*Figure 13*) would help dampen out movement of the model. A thin piece of plexiglas was used in covering the opening but it noticeably absorbed some of the object wave energy.

It should be noted that the acoustical transducers had to be reconditioned. Both transducers were full of immersion fluid from the main tank and as a result did not function properly. The object transducer's inside coating was half gone. The inside coating on one side had flaked off from the crystal. The remaining coating was removed on the inside and a gold coating was deposited. Both transducers were then sealed with a black silicone rubber sealant (*Figure 15*). The transducers have functioned properly since.

Part of this work was centered around attempting to develop a thermoplastic memory device for storing acoustical holograms. The potential of storing acoustical images would open the possibility of using double exposures and quantifying model displacements, internal to the surface as well as on the surface. Eventually this could assist in evaluating surface strains and even subsurface strains. The potential for doing this looks promising even though little apparent success was realized. This technique has been used in optical holography with success and it would appear the techniques could be readily adapted to acoustical holography. Essentially the mechanism for doing this is to have a thermoplastic film in contact with the immersion fluid. At a specified time the film would be heated and softened, allowing the acoustical energy to deform the thermoplastic surface into a holographic diffraction pattern, as is done on the water surface without the film. Next the thermoplastic would be allowed to cool and "lock" in the diffraction pattern for use as a permanent hologram.

Several devices were made and tried. An example of one device is shown in *Figure 16*. A four inch by four inch by .05 inch piece of glass has been coated with indium oxide so current could be passed through the layer. Copper bars were attached to the indium coating with a conducting epoxy. These bars distributed the current so it would flow through the coating. A dam was made of silicone rubber so that thermoplastic could be flowed on the indium oxide coating. The device was leveled. Thermoplastic was dissolved in hexane and poured into the reservoir formed by the silicone rubber dam. When the hexane evaporated, the thermoplastic was distributed over the indium oxide surface. Devices with thermoplastic thicknesses of 0.001, 0.002, 0.003, 0.005 and 0.010 inch were made. The thermoplastic thickness was controlled by knowing the area of the reservoir and the density of the thermoplastic. There is a possibility that some of the thermoplastic was evaporated with the hexane. This, of course, could change the properties of the thermoplastic and would make the amount of hexane, in comparison to the thermoplastic, important. A 20 percent thermoplastic solution was used as well as much higher dilution ratios in some devices. The devices were mounted in the system so

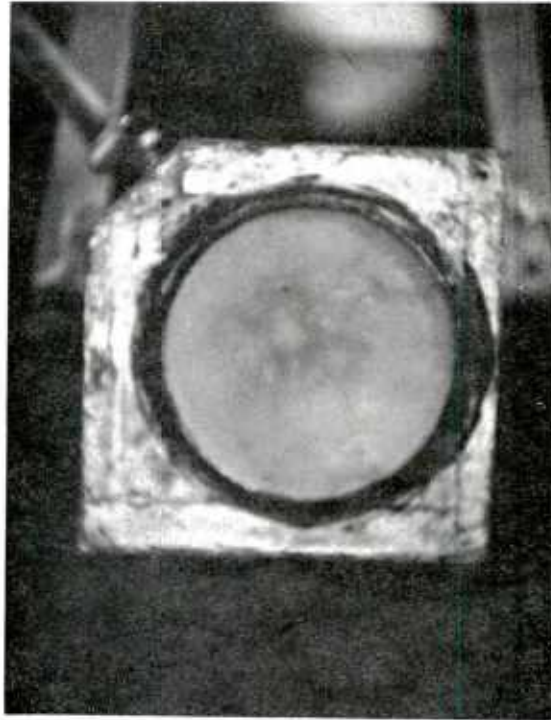


Figure 15. Sealed transducer.

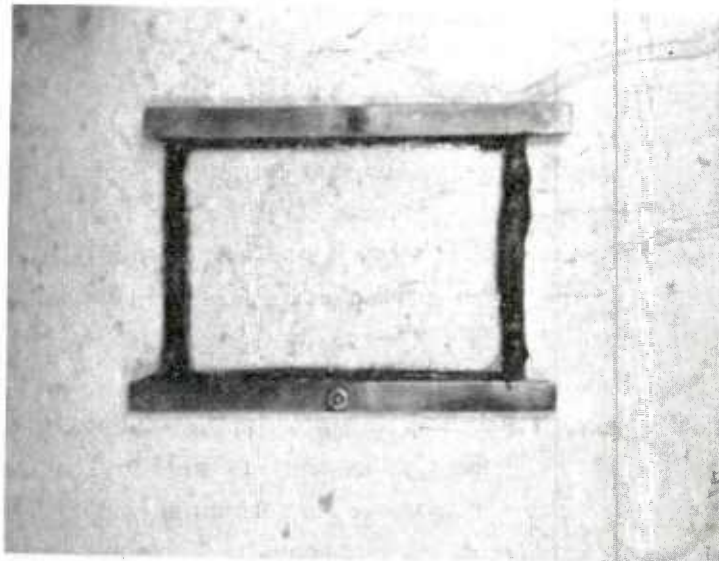


Figure 16. Resistance heated thermoplastic device.

that the thermoplastic surface was in contact with the water surface and at the water surface. Real time holograms were not apparent with this arrangement. Heat was applied to the device with electric circuits similar to the one illustrated and pictured in *Figure 17*. The temperature of the thermoplastic is very difficult to measure because of the thin layer; therefore, many different heating times were tried from ten milliseconds up to two minutes. The devices were removed and observed in a filter arrangement shown in *Figure 18*. In some instances some extremely questionable images were observed; but nothing that was definite and easily repeatable was seen. One of the biggest problems was obtaining a thermoplastic device with an optically smooth surface. This could have been caused by uneven evaporation of the hexane. After heating, the surface further optically deteriorated obscuring any possible diffraction pattern. This was probably caused by uneven heating and uneven cooling. There is the possibility of using a very thin layer of thermoplastic such as used in optical holography for correcting the uneven heating and cooling. Such a device was made but time was not available to try this approach. The device was made by dipping a plate into solution and carefully controlling the extraction rate. By weighing the device before and after dipping, the film thickness was estimated.

One thermoplastic device was made and heating and cooling applied with hot and cold water but no success was apparent.

Another device was made and is shown in *Figure 19*. This device floated on the surface of the water and was made of plexiglas. The thermoplastic layer was on the inside and was very thick (0.1 inch). The object wave had to pass through the plexiglas and then into the thermoplastic. In this manner a very poor outline could be seen of the test target bars. The reference beam was not received by the thermoplastic. In the arrangement used, the reference beam and plexiglas intersected at an angle greater than the critical angle; thus the reference beam was reflected. No diffraction orders, of course, would be seen. In this arrangement the surface of the thermoplastic was viewed in real time. Some heat was applied using a heat lamp to soften the thermoplastic. Another technique was to pour in a small amount of hexane and let it soften the surface and then evaporate. This was not successful.

An attempt was made at photographing the surface of the water and then filtering the film for the image. The filtering arrangement is illustrated in *Figure 20*. The filtered image of the test target is shown in *Figure 21*. The purpose for such an attempt was to suggest the possibility of doing double exposed holography with acoustics. The double exposure was not tried but with some work this would appear to be feasible. This would allow an investigator to quantify displacements of an object and maybe interior displacement.

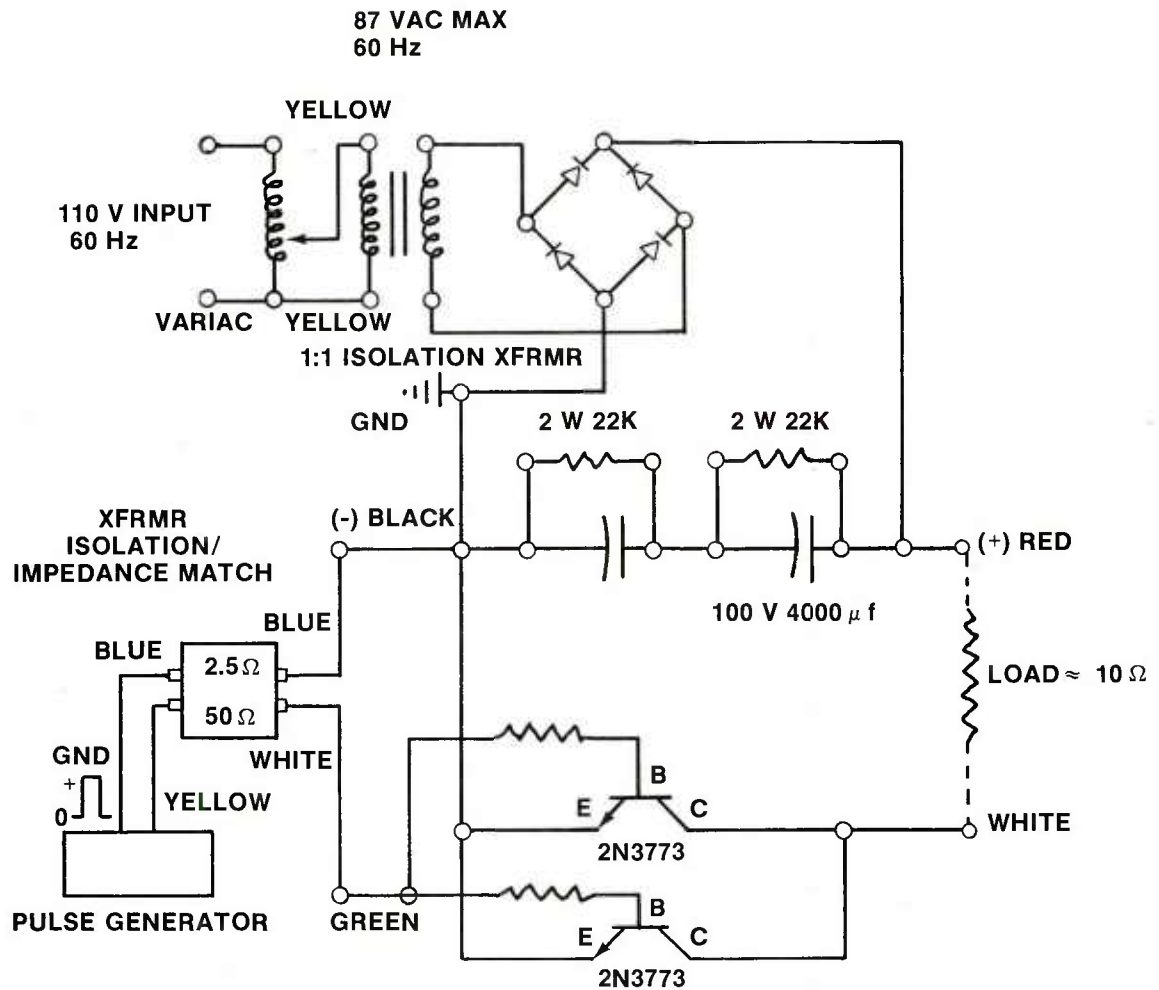


Figure 17. Resistance heating circuit.

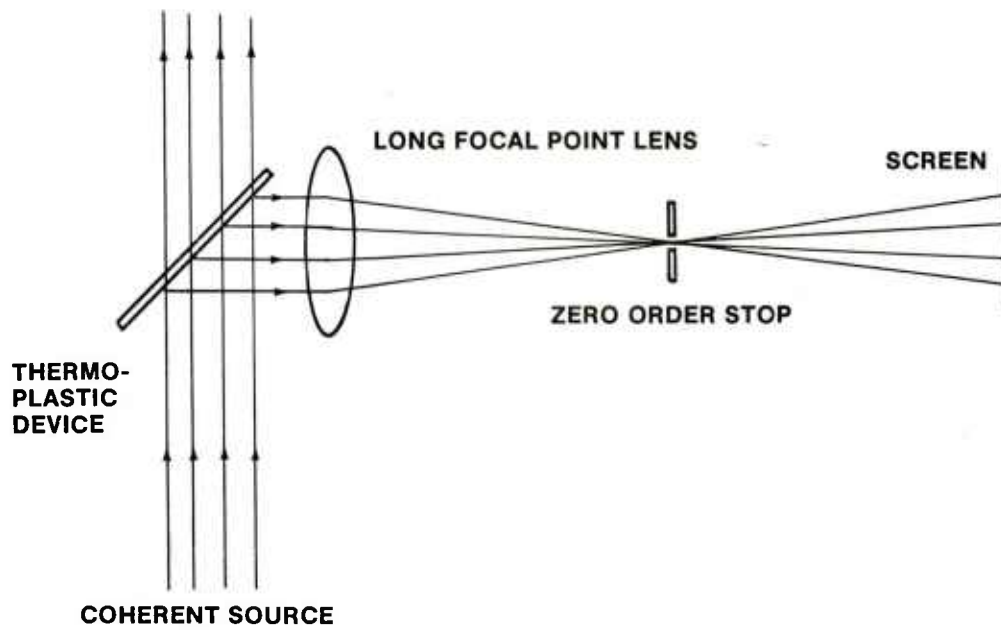


Figure 18. Filtered observation.



Figure 19. Floating thermoplastic device.

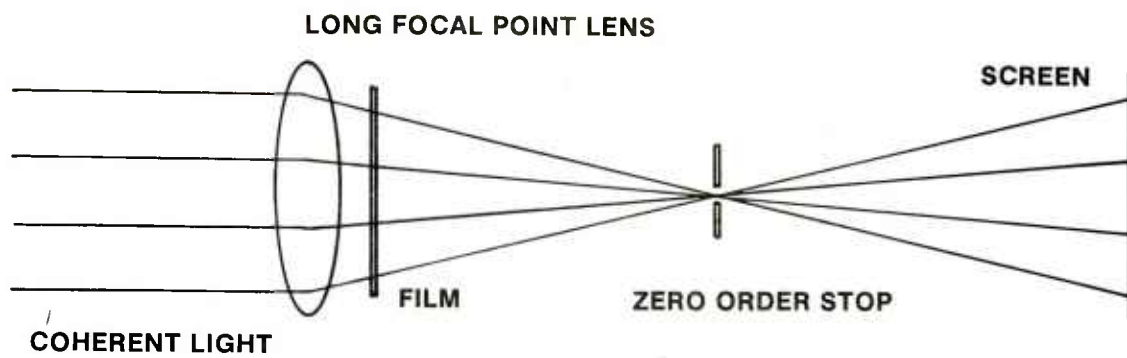


Figure 20. Film filter system.

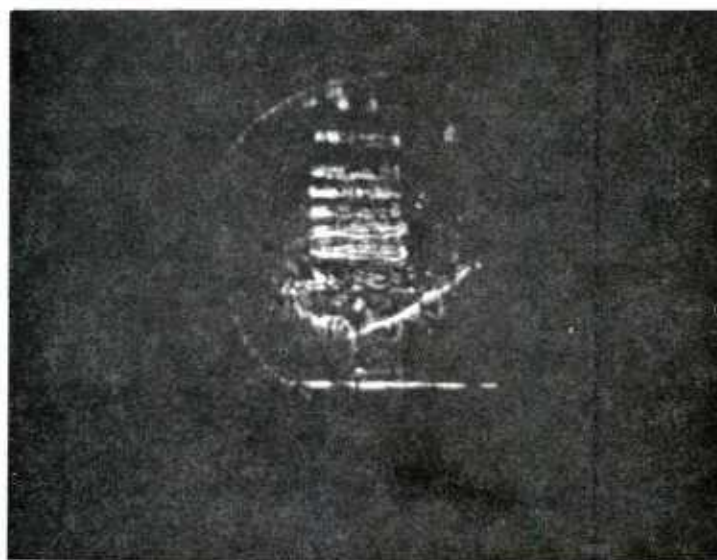


Figure 21. Film record.

An attempt was made to do speckle work with acoustics. A piece of clear plexiglas was inserted into the object beam path. No reference was used. A photograph was made of the water surface. Then the plexiglas was displaced 0.006 inch and a double exposure made. The film was examined using a laser beam of light. At some locations very distinct "Young's fringes" were observed, as shown in *Figure 22*. At other places nothing was observed and still other places strange patterns were seen. This looks very promising. It may require that instead of a laser to examine the film, an acoustic beam would be necessary. It does appear that displacements can be recorded in this manner.

IV. CONCLUSIONS AND RECOMMENDATIONS

The following conclusions and recommendations are made:

1. Pure glycerine as an acoustical immersion fluid is not suitable because of high surface tension. It is recommended that detergent be added to the glycerine and diluted with water as a possible immersion fluid.
2. Plexiglas is a good material for acoustical lenses.



Figure 22. Acoustical Young's fringes.

3. To improve the acoustical image further, it is recommended that the image be converted to digital form, filtered and enhanced, then converted back to analogue and displayed on a TV screen.
4. If tungsten steel is readily available an improved reflection can be made from this.
5. It is recommended that a thermoplastic memory device with very thin (less than 0.001 inch) coatings be investigated.
6. It is recommended that acoustical speckle be investigated as a possible technique to quantify surface and subsurface displacements.
7. It is recommended that the acoustical ripple pattern on the water surface be photographed using double exposure techniques for possibly recording displacement information.

DISTRIBUTION

	No. of Copies
Defense Technical Information Center Cameron Station Alexandria, Virginia 22314	12
Defense Metals Information Center Battelle Memorial Institute 505 King Avenue Columbus, Ohio 43201	1
Commander US Army Foreign Science and Technology Center ATTN: DRXST-SD3 220 Seventh Street, NE Charlottesville, Virginia 22901	1
Office of Chief of Research and Development Department of the Army ATTN: DARD-ARS-P Washington, DC 20301	1
Commander US Army Electronics Command ATTN: DRSEL-PA-P -CT-DT -PP, Mr. Sulkolove Fort Monmouth, New Jersey 07703	1 1 1
Commander US Army Natick Laboratories Kansas Street ATTN: STSNLT-EQR Natick, Massachusetts 01760	1
Commander US Army Mobility Equipment Research and Development Center Fort Belvoir, Virginia 22060	1

DISTRIBUTION (Continued)

	No. of Copies
Director USA Mobility Equipment Research and Development Center Coating and Chemical Laboratory ATTN: STSFB-CL Aberdeen Proving Ground, Maryland 21005	1
Commander Edgewood Arsenal ATTN: SAREA-TS-A Aberdeen Proving Ground, Maryland 21010	1
Commander Picatinny Arsenal ATTN: SARPA-TS-S, Mr. M. Costello Dover, New Jersey 07801	1
Commander Rock Island Arsenal Research and Development ATTN: 9320 Rock Island, Illinois 61201	1
Commander Watervliet Arsenal Watervliet, New York 12189	1
Commander US Army Aviation Systems Command ATTN: DRSAV-EE -MT, Mr. Vollmer St. Louis, Missouri 63166	1 1
Commander US Army Aeronautical Depot Maintenance Center (Mail Stop) Corpus Christi, Texas 78403	1
Commander US Army Test and Evaluation Command ATTN: DRSTE-RA Aberdeen Proving Ground, Maryland 21005	
Commander ATTN: STEAP-MT Aberdeen Proving Ground, Maryland 21005	1

DISTRIBUTION (Continued)

	No. of Copies
Chief Bureau of Naval Weapons Department of the Navy Washington, DC 20390	1
Chief Bureau of Ships Department of the Navy Washington, DC 20315	1
Naval Research Laboratory ATTN: Dr. M. M. Krafft Code 8430 Washington, DC 20375	1
Commander Wright Air Development Division ATTN: ASRC Wright-Patterson Air Force Base, Ohio 45433	1
Director Air Force Materiel Laboratory ATTN: AFML-DO-Library Wright-Patterson Air Force Base, Ohio 45433	1
Director Army Materials and Mechanics Research Center ATTN: DRXMR-PL -MT, Mr. Farrow Watertown, Massachusetts 02172	1 1
Commander White Sands Missile Range ATTN: STEWS-AD-L White Sands Missile Range, New Mexico 88002	1
Deputy Commander US Army Nuclear Agency ATTN: MONA-ZB Fort Bliss, Texas 79916	1
Jet Propulsion Laboratory California Institute of Technology ATTN: Library/Acquisitions 111-113 4800 Oak Grove Drive Pasadena, California 91103	1

DISTRIBUTION (Continued)

	No. of Copies
Sandia Laboratories ATTN: Library P O Box 969 Livermore, California 94550	1
Commander US Army Air Defense School ATTN: ATSA-CD-MM Fort Bliss, Texas 79916	1
Technical Library Naval Ordnance Station Indian Head, Maryland 20640	1
Commander US Army Materiel Development and Readiness Command ATTN: DRCMT Washington, DC 20315	1
Headquarters SAC/NRI (Stinfo Library) Offutt Air Force Base, Nebraska 68113	1
Commander Rock Island Arsenal ATTN: SARRI-KLPL-Technical Library Rock Island, Illinois 61201	1
Commander (Code 233) Naval Weapons Center ATTN: Library Division China Lake, California 93555	1
Department of the Army US Army Research Office ATTN: Information Processing Office P O Box 12211 Research Triangle Park, North Carolina 27709	1
ADTC (DLDSL) Eglin Air Force Base, Florida 32542	1

DISTRIBUTION (Continued)

	No. of Copies
University of California Los Alamos Scientific Laboratory ATTN: Reports Library P O Box 1663 Los Alamos, New Mexico 87545	1
Commander US Army Materiel Development and Readiness Command ATTN: DRCRD DRCDL 5001 Eisenhower Avenue Alexandria, Virginia 22333	1 1
Director Defense Advanced Research Projects Agency 1400 Wilson Boulevard Arlington, Virginia 22209	1
Commander US Army Research Office ATTN: DRXRO-PW, Dr. R. Lontz P O Box 12211 Research Triangle Park, North Carolina 27709	2
US Army Research and Standardization Group (Europe) ATTN: DRXSN-E-RX, Dr. Alfred K. Nodoluha Box 65 FPO New York 09510	2
Headquarters Department of the Army Office of the DCS for Research Development and Acquisition Room 3A474, The Pentagon ATTN: DAMA-ARZ Washington, DC 20310	2
US Army Materiel Systems Analysis Activity ATTN: DRXSY-MP Aberdeen Proving Ground, Maryland 21005	1
IIT Research Institute ATTN: GACIAC 10 West 35th Street Chicago, Illinois 60616	1

DISTRIBUTION (Concluded)

	No. of Copies
DRSMI-LP, Mr. Voigt	1
DRSMI-R, Dr. Kobler	1
-RL, Mr. Lewis	1
-RLA, Mr. Pettey	1
-RLA, Dr. Mullinix	1
Mr. Schaeffel	50
-RT	1
-ICBB	1
-RPR	3
-RPT (Record Set)	1
(Reference Copy)	1